Supporting Information

Highly Flexible Honeycomb-structured Flexible Transparent Conductive Electrodes by Inkjet printing for Light-Emitting Devices

Chuang Liu[1,2,3], Haoran Quan[1,2,3], Yangliu Shi[1,2], Hongyan Chen[1,2,3], He Dong[1,2,3], JintaoWang[4], Ye Tao[5], Chen Chen[1,2,3],* and Jin Wang[1,2,3]*

1. College of Information Technology, Jilin Engineering Research Center of Optoelectronic Materials and Devices, Jilin Normal University, Siping 136000, China .
2. Jilin Provincial Key Laboratory of Wide Bandgap Semiconductor Material Growth and Device Applications, Jilin Normal University, Changchun 130103, China.
3. Key Laboratory of Functional Materials Physics and Chemistry of the Ministry of Education, Jilin Normal University, Changchun 130103, China.
4. School of Information Engineering Yantai Institute of Technology, Yantai, 261400, China.
5. Liangjiang Institute of Artificial Intelligence, Chongqing University of Technology，Chongqing 400054, China.

Materials. Conductive silver paste NPS-J was purchased from SIJ in Japan, Poly(methyl methacrylate) average M.W. 15,000 (PMMA) was purchased from Beijing Bailing Wei Technology Co, Anisole (AR, 99%) was purchased from Rhawn Chemical Reagents, Isopropyl alcohol (IPA, >99.9%) purchased from Advanced election Technology, polyethylenedioxythiophene (Sodium styrene sulfonate) (PEDOT:PSS 4083) purchased from Xi 'an Yuri Solar Co, LTD, molybdenum trioxide (MoO_3),N,N′-Di(1-naphthyl)-N,N′-diphenyl-(1,1′-biphenyl)-4,4′-diamine(NPB),Tris(8-hydroxyquinoline)aluminum(III) (Alq_3) , 8 - Hydroxyquinolinolato - lithium (Liq) were purchased from Taiwan Lumtec Optical Technology Co. LTD. All materials are used as received and no further purification is required.

Film and Device Characterization. The following apparatus was utilized in the present study: a field emission scanning electron microscope (Hitachi S-4800) was employed to characterize the surface morphology of the electrodes. The transmittance of the electrodes in the visible region was characterized using a UV-Vis-NIR spectrophotometer (Shimadzu UV-3101PC). The contact angle of silver ink in the presence/absence of anhydrous sacrificial layer was characterized using an Ossila contact angle tester. The characterization of the silver nano-electrode films was conducted using a ray diffractometer (Rigaku D/max-ga X) at room temperature. The square resistance value and resistivity of the electrodes were measured using a handheld four-probe tester (Suzhou Jingge M-6). The flexible bending properties of the electrodes were then tested using a Flexible Device Cyclic Bending Test System (PURI MATERIALS PR-BDM), and the number of bends and changes in resistivity values during the test period were recorded. The current density-voltage-brightness characteristics of the OLEDs were recorded using a digital source meter (Keithley 2400) and a spectrometer (Spectra Scan PR-735). It is also noteworthy that all measurements were conducted under ambient atmospheric conditions.

Parameters of abaqus simulation. The silver grid structure in the simulation part of this paper has a Young's modulus of 71 GPa and a Poisson's ratio of 0.37, and the PMMA has a Young's modulus of 3.16 GPa and a Poisson's ratio of 0.32. The grid structure cell side length is 10, and the honeycomb structure cell side length is 8.8 (according to the experimental pattern design scale). Boundary conditions: U1 = U3 = UR1 = UR2 = UR3 = 0, U2 = -40.

Table S1 FTCEs reported in recent years.

Materials	Substrate	Resistivity	Transmittance	Flexibility	Ref.
AgNWs	PET	32Ω/sq	76.5%	9%/200 cycles	1
$Ti_3C_2T_x$/AgNWs/PEDOT	PET	29.9Ω/sq	81.1%	---	2
AgNWs	PET	26.5Ω/sq	95.2%	2.96%/1000 cycles	3
GP/AgNWs/HPMC	PET	4.2Ω/sq	81.5%	---	4
MXene/AgNWs	PMMA	13.9Ω/sq	83.8%	---	5
AgNWs/Propolis	PET	~15Ω/sq	~93%	---/10000 cycles	6
MoO_3/Au/MoO_3	NOA63	~15Ω/sq	~76%	---/1000 cycles	7
AgNPs	PMMA	11.27Ω/sq	86.44%	5.53%/70000 cycles	Here

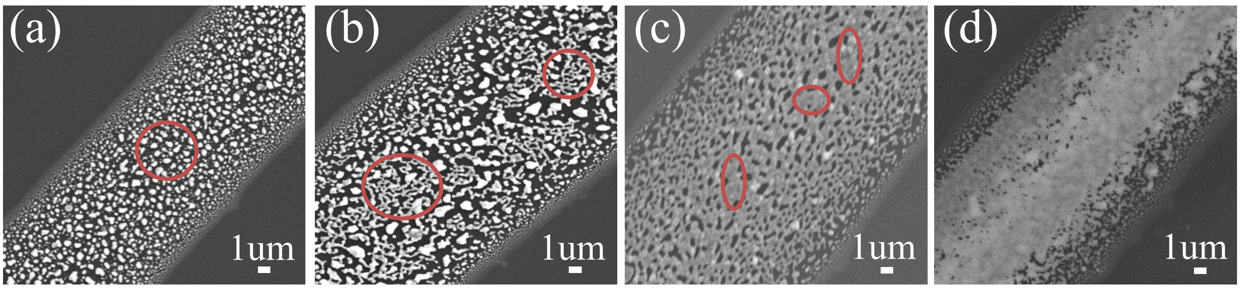

Figure. S1 (a-d) SEM image of silver nanoparticle arrangement in the line after 1-4 times of inkjet printing.

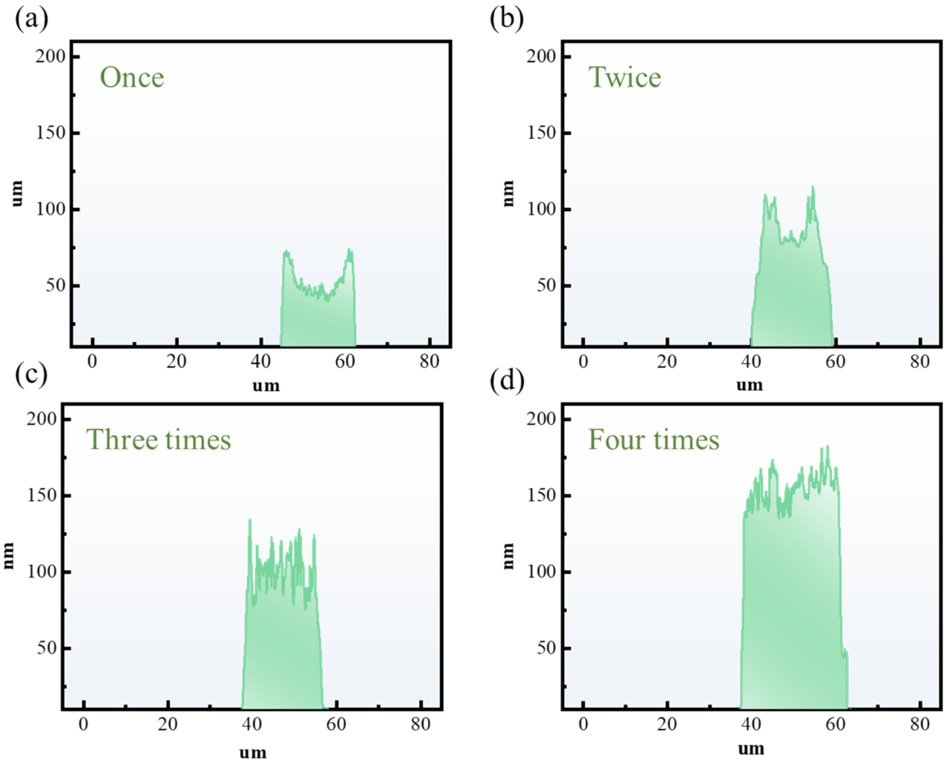

Figure. S2 Step profiler test for lines printed once to four times.

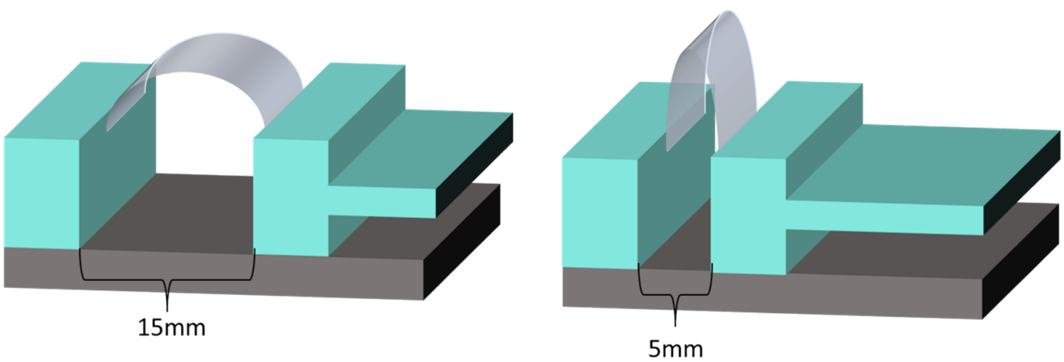

Figure. S3 Schematic diagram of cyclic bending test.

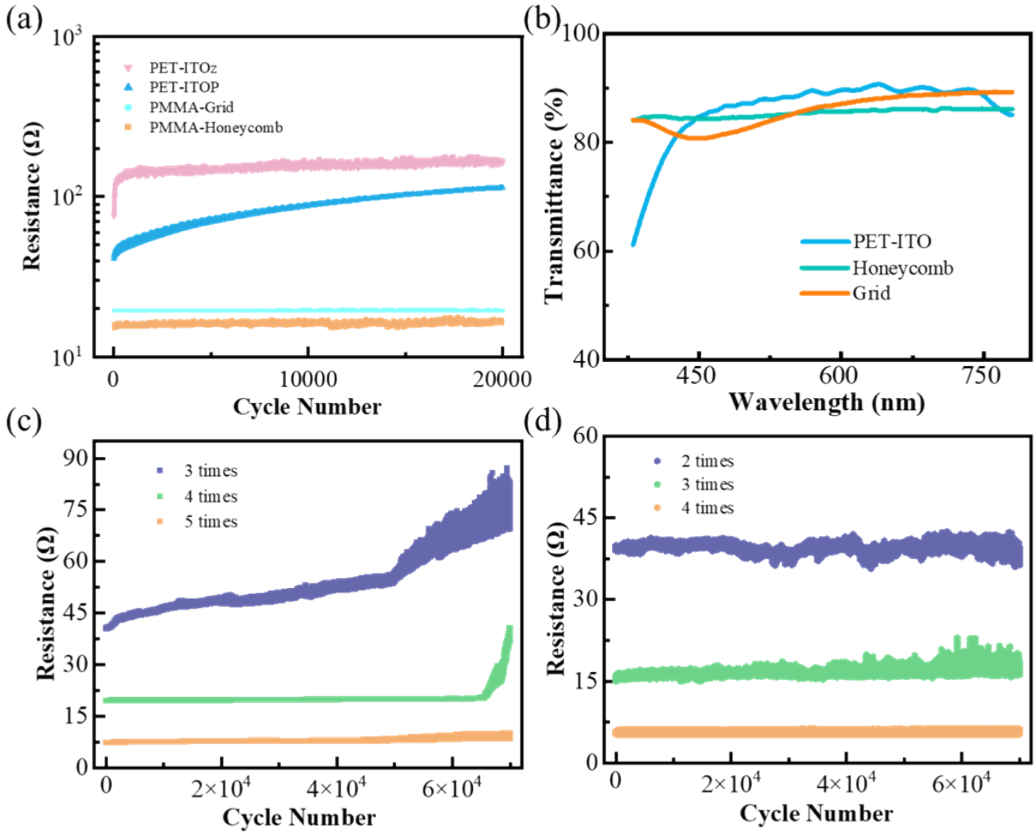

Figure. S4 (a) Resistance change of FTCEs with optimum number of prints versus commercially available PET-ITO in bending test. (b) Transmittance of FTCEs vs. commercially available PET-ITO for optimal number of prints. (c-d) Resistance variations in bending tests for grid-structured and honeycomb-structured FTCEs printed three times.

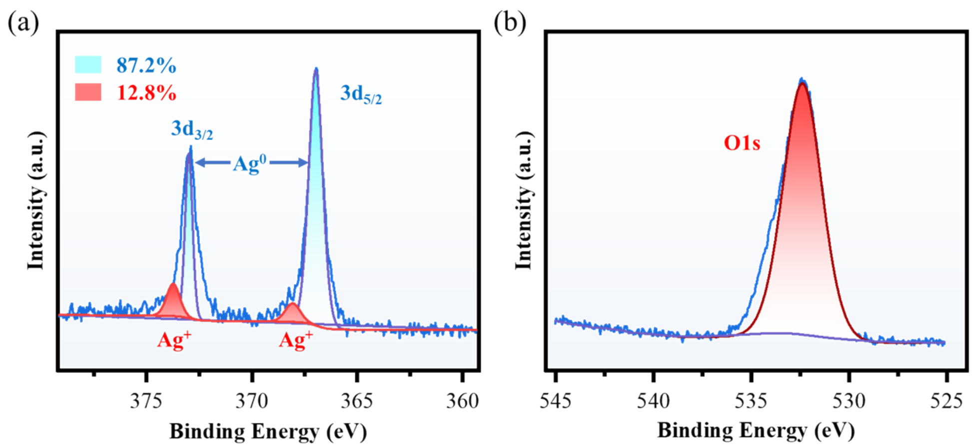

Figure. S5 XPS image of silver electrode after 70,000 cycles of bending test.

Reference：

1 S. Y. Wang, X. L. Wu, J. X. Lu, Z. W. Luo, H. Xie, X. B. Zhang, K. W. Lin and Y. H. Wang, *Nanomaterials,* 2022, **12**

2 Y. Z. Wang, Y. Liu, T. Wang, S. H. Liu, Z. Chen and S. B. Duan, *Nanotechnology,* 2022, **33**

3 M. Y. Du, Z. Yang, Y. Q. Miao, C. Wang, P. Dong, H. Wang and K. P. Guo, *Adv. Funct. Mater.,* 2024, **34**

4 P. F. Qian, W. H. Geng, Z. L. Bao, L. C. Jing, D. Zhang and H. Z. Geng, *Surfaces and Interfaces,* 2025, **56**

5 W. Jiang, S. Lee, K. Zhao, K. Lee, H. Han, J. Oh, H. Lee, H. Kim, C. M. Koo and C. Park, *Acs Nano,* 2022, **16**

6 Y. Qin, L. Q. Yao, F. B. Zhang, R. Q. Li, Y. J. Chen, Y. H. Chen, T. Cheng, W. Y. Lai, B. X. Mi, X. W. Zhang and W. Huang, *ACS Appl. Mater. Interfaces,* 2022, **14**, 38021-38030.

7 K. J. Ko, H. W. Cho, H. B. Lee, J. W. Kang, S. Y. Ryu and P. J. Jesuraj, *Org. Electron.,* 2024, **128**